Sensors and Materials, Vol. 32, No. 4 (2020) 1567–1576
MYU Tokyo

S & M 2202

Waveguide-mode Sensor Chip with $Si/SiO_2/SiO_x$ Structure

Masato Yasuura,[1*] Koji Ueno,[2] Hiroki Ashiba,[1] Yuki Nakaya,[1] and Makoto Fujimaki[1]

[1]Sensing System Research Center, National Institute of Advanced Industrial Science and Technology (AIST), Central 5, 1-1-1 Higashi, Tsukuba, Ibaraki 305-8565, Japan
[2]C&I Co., Ltd., 2004-1 Tamatori, Tsukuba, Ibaraki 300-3255, Japan

(Received December 12, 2019; accepted March 5, 2020)

Keywords: microcrystalline silicon, near-field light enhancement, sputtering deposition, transfer matrix method, refractive index measurement

A waveguide-mode sensor detects changes in the complex refractive index on the surface of a planar waveguide chip with high sensitivity. We developed a waveguide-mode sensor chip with the Si/SiO_2 structure. It was predicted from simulations that a third layer of high refractive index added to the outermost surface of the planar waveguide may improve the sensitivity of the waveguide-mode sensor. In this research, we designed and manufactured a borosilicate glass substrate chip with a $Si/SiO_2/SiO_x$ structure via sputtering deposition, and we improved the sensitivity of the waveguide-mode sensor chip. The $Si/SiO_2/SiO_x$ structure chip was approximately 1.5 times more sensitive to refractive index changes than the Si/SiO_2 structure chip.

1. Introduction

Various fields, such as the medical and pharmaceutical fields, require highly sensitive biological substance detection technology. The enhancement of electric fields of evanescent light, such as that used in surface plasmon resonance sensors, is a widely applied method for realizing highly sensitive detection.[1–3] The excitation of waveguide modes is one way to obtain an enhanced electric field of evanescent light.[4–6] A waveguide mode sensor detects changes in the complex refractive index on a planar waveguide surface made from stacked thin films, through electric field enhancement by multiple reflections at a specific wavelength.[5–8] For wavelengths with an enhanced electric field, a decrease in reflectance occurs and appears as a dip in the reflectance spectrum. When the refractive index on a waveguide surface increases, the dip position shifts toward the longer wavelength side. Using this property of the waveguide-mode, various substances, such as proteins, viruses, and biomarkers, adsorbed on the waveguide surface can be detected with high sensitivity.[9–15] Waveguide-mode sensors using a planar waveguide, with single-crystalline Si (c-Si) and SiO_2 layers sequentially stacked on a silica glass substrate, have been developed.[5,9–11] However, the waveguide-mode sensor chip fabricated using the silica glass substrate is expensive for commercial use. Inexpensive optical glass, such as borosilicate glass, is desirable for use as a substrate, but borosilicate glass has a drawback in

*Corresponding author: e-mail: yasuura-masato@aist.go.jp
https://doi.org/10.18494/SAM.2020.2732

ISSN 0914-4935

that its refractive index is higher than that of silica glass. If the refractive index of the substrate becomes higher, the sensitivity becomes worse.

In this study, numerical simulations predicted that increasing the refractive index n of the material of the outermost surface of a planar waveguide improves the sensitivity of the device, which can compensate for the drawback of borosilicate glass. To prove this prediction, we developed a sensor chip having an additional high-refractive-index layer. As an example of the material for the high-refractive-index layer, we chose SiO_x whose refractive index is higher than that of SiO_2. We designed and fabricated planar waveguides with the three-layer structure of μc-Si/SiO_2/SiO_x, and examined the performance of the waveguide-mode sensor.

For the fabrication of a Si/SiO_2 stacked film structure on an optical glass substrate, radio frequency (RF) magnetron sputtering is a desirable fabrication method.[16–18] Several techniques have been reported for forming an amorphous Si (a-Si) or a microcrystalline Si (μc-Si) at low temperatures that can be adopted for optical glass substrates having a low strain point, such as borosilicate glass.[17,18]

2. Materials and Methods

2.1 Fabrication of planar waveguides

Figure 1 shows the schematic of the optical system of the waveguide-mode sensor based on a parallel-incident-type sensor.[11] Borosilicate glass (BK-7) with a trapezoidal prism shape was used as the substrate of the sensor chip. The base angle on the upper base side of the substrate was 35°. The upper base length, width, and height of the substrate were 21, 8, and 2 mm, respectively. A RF magnetron sputtering device (i-miller, CFS-4EP-LL, Shibaura Mechatronics Corporation, Japan) was used to fabricate the waveguide-mode sensor chip. Si (99.999%, Kyodo International Inc., Japan) was used as the target for μc-Si film deposition. The sputter deposition of μc-Si was performed under an atmosphere of Ar and H_2 with flow rates of 8 and 12 sccm, respectively. SiO_2 (99.99%, Kyodo International Inc., Japan) was used as the target for SiO_2 film deposition. The sputter deposition of SiO_2 was performed under an atmosphere

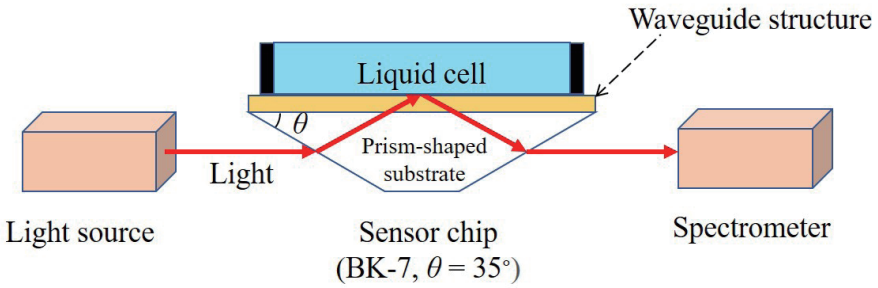

Fig. 1. (Color online) Schematic of optical system of waveguide-mode sensor. The optical system is based on a parallel-incident-type waveguide-mode sensor.[11] The symmetrical trapezoidal prism-shaped sensor chip is made of BK-7. The base angle θ on the upper base side of the sensor chip is 35°, and the liquid cell is filled with sample solutions of water or aqueous sodium chloride. White LEDs were used as the light source.

of Ar and O_2 with flow rates of 9 and 1 sccm, respectively. SiO (99.9%, Kyodo International Inc., Japan) and SiO_2 were used as the targets for SiO_x film deposition. The sputter deposition of SiO_x was performed under an atmosphere of Ar and H_2 with flow rates of 15 sccm for both gases. In each sputtering process, the initial pressure was 1.5×10^{-3} Pa, and the temperature of the heater for the stage on which the substrates were fixed was 300 °C. The refractive index n and extinction coefficient k of each sputter-deposited layer were measured using a spectroscopic ellipsometer (UVISEL, M200-FUV-FGMS-HNSTSS, HORIBA Jobin Yvon GmbH, Germany).

2.2 Evaluation of fabricated waveguide-mode sensor chip

The sensitivity of the fabricated waveguide-mode sensor chips was evaluated using a waveguide-mode sensor (Eva-M02, C&I Co., Ltd., Japan). The incident light, whose direction was parallel to the bottom surface of the sensor chip, was irradiated onto the waveguide structure deposited on the prism-shaped sensor chip (see Fig. 1). The light was reflected and diffracted at each boundary of the layers in the waveguide structure and totally reflected at the chip surface. A dip was observed where the wavelength in the spectrum of the reflected light directed to the spectrometer has a lower reflectance, which was due to the optical absorption by the Si layer. The dip shifted to the longer-wavelength side owing to the increase in the refractive index at the chip surface.[7,11]

The experimental procedure for evaluating the performance of the fabricated sensor chips was as follows. First, pure water was introduced into the liquid cell formed on the fabricated sensor chip, and the reflection spectrum was measured using the spectrometer. Next, sodium chloride aqueous solution was introduced into the liquid cell, and the reflection spectrum was measured. The liquid cell was washed three times with pure water.

3. Theoretical Simulation

The model of the optical system used for the simulation of the electric field is shown in Fig. 1. The waveguide structure models of the Si/SiO_2 and $Si/SiO_2/SiO_x$ waveguide-mode sensor chips are shown in Fig. 2. The results of complex refractive index measurements by ellipsometry are shown in Fig. 3. Figures 3(a)–3(c) show the results of μc-Si, SiO_2, and SiO_x, respectively. Table 1 shows the complex refractive indices of the fabricated Si layer and those of the a-Si and μc-Si films reported in Refs. 19 and 20, respectively. As shown in Fig. 3(a) and Table 1, the k values of the fabricated Si layer were similar to those of μc-Si and lower than those of a-Si reported in the references.

Using the obtained complex refractive indices of μc-Si, SiO_2, and SiO_x and the referenced complex refractive indices of c-Si and a-Si,[19,21] Si/SiO_2 and $Si/SiO_2/SiO_x$ planar waveguide structures for waveguide-mode sensors were designed. In this study, the planar waveguide structures were optimized to enhance the electric field of light with a wavelength of 650 nm. The outermost surface was assumed to be in contact with water. The simulation was performed using the transfer matrix method for a stratified medium using the Fresnel equations [see Eq. (1)].[22]

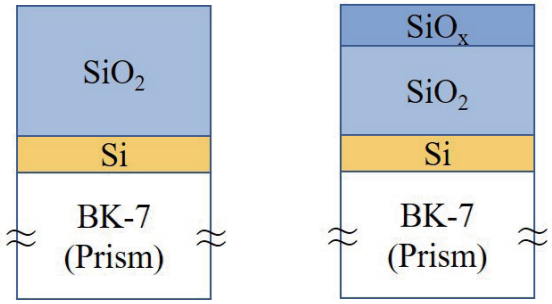

Fig. 2. (Color online) Si/SiO_2 and $Si/SiO_2/SiO_x$ planar waveguide structure models. (a) A Si layer and a SiO_2 layer are sequentially stacked on a BK-7 glass substrate. (b) A Si layer, a SiO_2 layer, and a SiO_x layer are sequentially stacked on a BK-7 glass substrate.

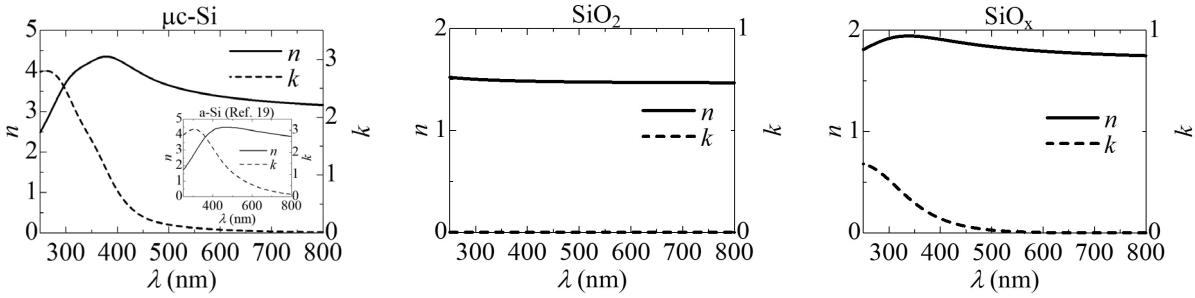

Fig. 3. Complex refractive indices obtained via ellipsometry. The n and k values of (a) μc-Si, (b) SiO_2, and (c) SiO_x are indicated by solid and broken lines, respectively. The inset of Fig. 3. (a) shows the complex refractive indices of the a-Si film reported in Ref. 19.

Table 1
Complex refractive indices values of the Si layer at wavelength of approximately 650 nm.

	n	k	
Fabricated Si	3.32	0.04	@ 636 nm
a-Si	4.17	0.36	@ 653 nm (Ref. 19)
μc-Si	3.86	0.03	@ 633 nm (Ref. 20)

$$t_s = \frac{2\sin\beta\cos\alpha}{\sin(\alpha+\beta)},\ r_s = -\frac{\sin(\alpha-\beta)}{\sin(\alpha+\beta)}, \tag{1}$$

where α is the incident angle, β is the reflection angle, t_s and r_s are the transmission and reflection coefficients of s polarized light, respectively.

For the simulations, a conventional Si/SiO_2 waveguide structure was first designed. The enhancement factor of the electric field at the waveguide–water interface as a function of the Si and SiO_2 layer thicknesses is shown in Fig. 4. Figures 4(a)–4(c) show the results of the calculations using the c-Si, a-Si, and μc-Si films as the Si layer, respectively. Table 2 shows the

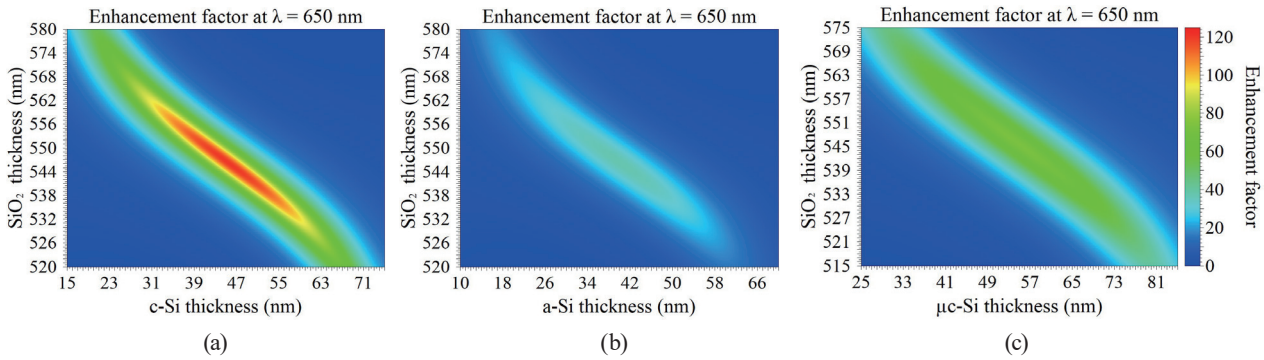

Fig. 4. (Color online) Enhancement factors of Si/SiO_2 structure chips at wavelength of 650 nm. The enhancement factor indicates the electric field intensity, assuming that the electric field intensity of the incident light is 1. The enhancement factors of the electric field at the waveguide–water interface are calculated. The Si and SiO_2 layer thicknesses of the Si/SiO_2 waveguide structure are indicated on the *x*- and *y*-axes, respectively. The (a) c-Si, (b) a-Si, and (c) μc-Si films are used as the Si layer.

Table 2
Highest enhancement factors and layer thicknesses of the Si/SiO_2 structure chips at wavelength of 650 nm.

	Si layer (nm)	SiO_2 layer (nm)	Enhancement factor
c-Si	45	546	120
a-Si	40	546	37
μc-Si	54	546	73

highest enhancement factors of the simulated c-Si/SiO_2, a-Si/SiO_2, and μc-Si/SiO_2 waveguides. The Si and SiO_2 layer thicknesses in each chip are summarized in Table 2. Next, a $Si/SiO_2/SiO_x$ waveguide structure was designed. The result of the calculation of the enhancement factor as a function of the SiO_2 and SiO_x layer thicknesses is shown in Fig. 5. Figures 5(a)–5(c) show the results of the calculations using the c-Si, a-Si, and μc-Si films as the Si layer, respectively. The Si layer thicknesses were fixed at values shown in Table 2. Table 3 shows the highest enhancement factors of the simulated c-$Si/SiO_2/SiO_x$, a-$Si/SiO_2/SiO_x$, and μc-$Si/SiO_2/SiO_x$ waveguides, and the Si, SiO_2, and SiO_x layer thicknesses.

Figure 6 shows the simulations of the dip wavelength changes $\Delta\lambda$ with the refractive index change Δn. The values of $\Delta\lambda$ was obtained by subtracting the dip wavelength of the reflection spectrum in the measurement with the NaCl solution from that in the measurement with pure water. The calculation results of the designed Si/SiO_2 and $Si/SiO_2/SiO_x$ structure chips are indicated by solid and broken lines, respectively. As shown in Fig. 6, the slopes of the designed c-Si/SiO_2, a-Si/SiO_2, and μc-Si/SiO_2 structure chips at $\Delta n = 0$ were all 850 nm/RIU, where RIU stands for the refractive index unit. The slopes of the designed c-$Si/SiO_2/SiO_x$, a-$Si/SiO_2/SiO_x$, and μc-$Si/SiO_2/SiO_x$ structure chips at $\Delta n = 0$ were all 1250 nm/RIU. The designed $Si/SiO_2/SiO_x$ structure chips were 1.47 times more sensitive than the designed Si/SiO_2 structure chips to the refractive index changes Δn. By adding a high-refractive-index material layer, the sensitivity of the waveguide-mode sensor to the refractive index changes is expected to improve.

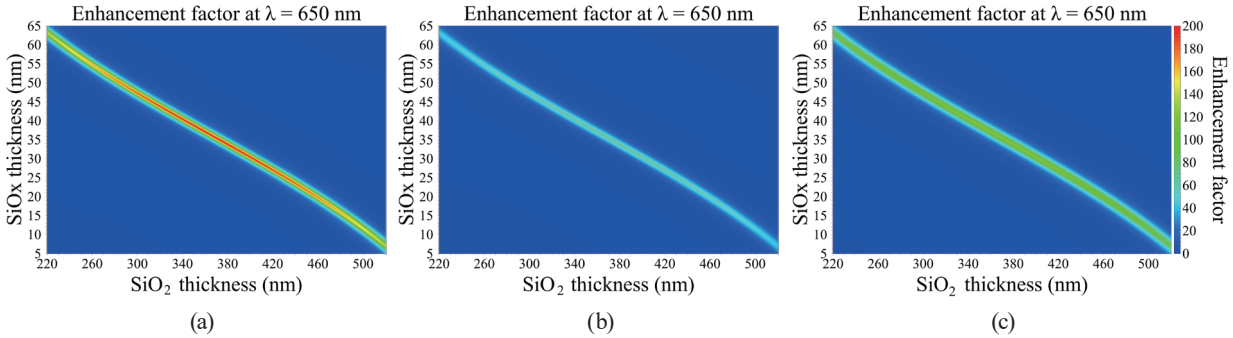

Fig. 5. (Color online) Enhancement factors of $Si/SiO_2/SiO_x$ structure chips at wavelength of 650 nm. The enhancement factor indicates the electric field intensity, assuming that the electric field intensity of the incident light is 1. The enhancement factors of the electric field at the waveguide–water interface are calculated. The SiO_2 and SiO_x layer thicknesses of the $Si/SiO_2/SiO_x$ waveguide structure are indicated on the *x*- and *y*-axes, respectively. The (a) c-Si, (b) a-Si, and (c) μc-Si films are used as the Si layer.

Table 3
Highest enhancement factors and layer thicknesses of the $Si/SiO_2/SiO_x$ structure chips at wavelength of 650 nm.

	Si layer (nm)	SiO_2 layer (nm)	SiO_x layer (nm)	Enhancement factor
c-Si	45	369	36	198
a-Si	40	367	36	62
μc-Si	54	369	36	122

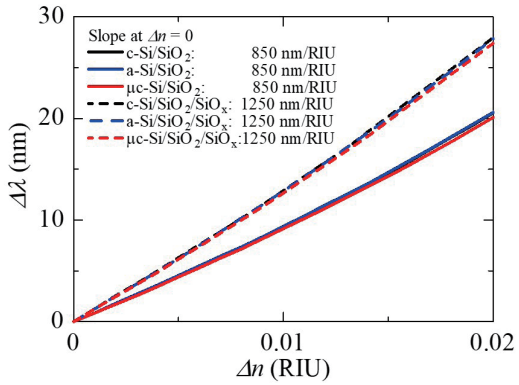

Fig. 6. (Color online) Theoretical performance of designed Si/SiO_2 and $Si/SiO_2/SiO_x$ structure chips. The slopes of the three types of Si/SiO_2 structure chip were almost identical. The slopes of the three types of $Si/SiO_2/SiO_x$ structure chip were almost identical. The slope ratio of the Si/SiO_2 chip to that of the $Si/SiO_2/SiO_x$ structure chip was 1.47.

4. Results

Figure 7 shows the reflectance spectra obtained when pure water was measured and the dip wavelength changes $\Delta\lambda$ observed when the sodium chloride solutions were measured. The dip wavelengths of the fabricated μc-Si/SiO_2 and μc-$Si/SiO_2/SiO_x$ structure chips in the pure water measurement were 658.9 ± 6.4 and 651.9 ± 6.5 nm, respectively. The refractive indices

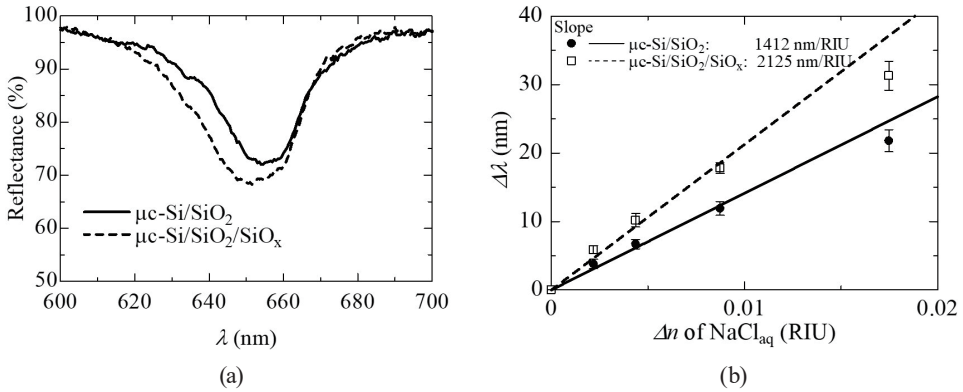

Fig. 7. (a) Reflectance spectra of fabricated μc-Si/SiO_2 and μc-Si/SiO_2/SiO_x structure chips obtained when pure water was measured. (b) Changes in dip positions when sodium chloride solutions were measured using fabricated chips. The solid and dotted lines are drawn by least-squares fitting to the obtained results. The slope of the μc-Si/SiO_2/SiO_x structure chip was 1.5 times larger than that of the μc-Si/SiO_2 structure chip.

of the sodium chloride solutions were measured using an Abbe refractometer. The linear approximations of the results of the fabricated μc-Si/SiO_2 and μc-Si/SiO_2/SiO_x structure chips obtained by the least-squares method are indicated by solid and broken lines, respectively. As shown in Fig. 7, the slopes of the linear approximations of the fabricated μc-Si/SiO_2 and μc-Si/SiO_2/SiO_x structure chips were 1412 and 2125 nm/RIU, respectively. The fabricated μc-Si/SiO_2/SiO_x structure chip was 1.5 times more sensitive than the fabricated μc-Si/SiO_2 structure chip to the refractive index changes Δn.

5. Discussion

As shown in Figs. 6 and 7, the $\Delta\lambda/\Delta n$ slopes of the Si/SiO_2/SiO_x structure chips were approximately 1.5 times those of the Si/SiO_2 structure chips in both theoretical and experimental results. The deposition of the third layer with a high refractive index is effective in improving the sensitivity of the waveguide-mode sensor. The $\Delta\lambda/\Delta n$ slopes of the fabricated μc-Si/SiO_2 and μc-Si/SiO_2/SiO_x structure chips were approximately 1.7 times larger than those of the designed chips in the simulations. This might be caused by the unevenness of the fabricated chip surfaces. Unlike the ideally flat surface assumed in the simulations, the sputter-deposited surfaces have irregularities. Nanoholes in the waveguide structure surface can effectively enhance the sensitivity of the waveguide-mode sensor.[9] The unevenness of the fabricated chip surfaces might similarly enhance the sensitivity of the waveguide-mode sensor. The standard deviation of the dip wavelength with respect to pure water of the three-layer waveguide structure chips was less than 1%, and the dip wavelength did not change for two months (data not shown). These results indicate that the reproducibility and stability of the fabricated SiO_x layer is good enough for practical use.

In this study, we investigated and developed sensor chips having an outermost SiO_x layer. Such higher sensitivity can be obtained regardless of the material of the third layer as long as the material has a higher refractive index than SiO_2. Figure 8 shows calculation result of $\Delta\lambda$

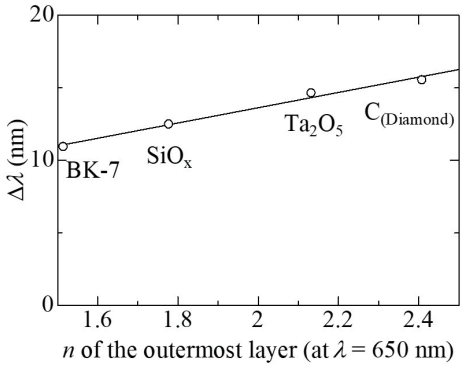

Fig. 8. Calculation result of $\Delta\lambda$ of waveguide-mode sensor with refractive index of outermost layer, where Δn of solution was assumed to be 0.01. The thickness of the Si layer was 54 nm. The thicknesses of the outermost layer and the SiO_2 layer were optimized to make the sensor having the initial dip position of 650 nm and to maximize the $\Delta\lambda$ for each material. The refractive indices of BK-7, SiO_x, Ta_2O_5, $C_{(Diamond)}$ are indicated by open circles.

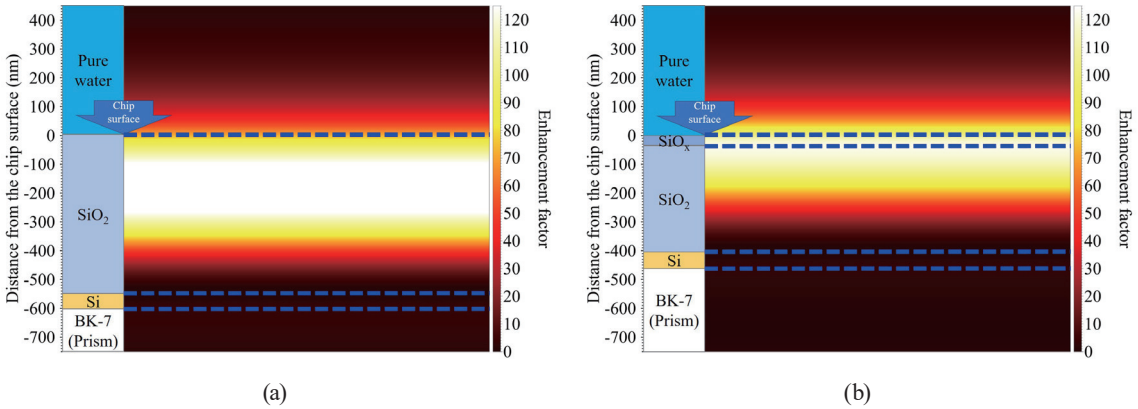

Fig. 9. (Color online) Intensities of enhanced electric field of (a) two-layer (μc-Si/SiO_2) and (b) three-layer (μc-Si/SiO_2/SiO_x) waveguides. The enhancement factor indicates the value of electric field intensity, assuming that the electric field intensity of incident light is 1. The interfaces of each layer of the waveguides are indicated by the blue broken lines. The thicknesses of layers are the same as those in Tables 2 and 3.

of the waveguide-mode sensor with the refractive index of the outermost layer, where Δn of the solution was assumed to be 0.01. In the calculation, the thickness of the Si layer was 54 nm. The thicknesses of the outermost layer and the SiO_2 layer were optimized to make the sensor having the initial dip position of 650 nm and to maximize the $\Delta\lambda$ for each material. The refractive indices of BK-7, SiO_x, Ta_2O_5, $C_{(Diamond)}$ are indicated by open circles in Fig. 8. As shown in Fig. 8, $\Delta\lambda$ increases with increasing n of the outermost layer, indicating that a high-refractive-index material is desirable for the outermost layer.

Figures 9(a) and 9(b) show intensities of the enhanced electric field of the two-layer (μc-Si/SiO_2) and three-layer (μc-Si/SiO_2/SiO_x) waveguides. The distance from the chip surface of the waveguide structure and the enhancement factor of the electric field are indicated on the y-axis and color bar, respectively. The interfaces of each layer of the waveguides are indicated

by the blue broken lines. As can be seen, the outermost SiO_x layer makes the peak position of the enhanced electric field closer to the chip surface, and as a result, the intensity of the electric field at the surface of the three-layer waveguide is higher than that of the two-layer waveguide. It seems that the increase in the intensity of the electric field by the third layer improves the sensitivity of the waveguide-mode sensor.

6. Conclusions

In this study, we improved the sensitivity of waveguide-mode sensors with the $Si/SiO_2/SiO_x$ structure in which a high-refractive-index SiO_x layer is added to the outermost surface of a Si/SiO_2 structure waveguide. The sensitivities of the Si/SiO_2- and $Si/SiO_2/SiO_x$-structure waveguide-mode sensor chips using c-Si, a-Si, and μc-Si as the Si layers were compared through simulations. In all the cases, the $Si/SiO_2/SiO_x$ structure was 1.5 times more sensitive than the Si/SiO_2 structure in a waveguide-mode sensor chip. This result was in agreement with the experimental results obtained where the sensor chip was fabricated by the RF sputtering method. These results indicate that the addition of a high-refractive-index layer is an easy and effective way to improve the sensitivity of waveguide-mode sensors.

Acknowledgments

This work was partly supported by the JSPS KAKENHI [grant numbers 17H01048 and 18H01803]. Part of this work was conducted at the AIST Nano-Processing Facility, supported by "Nanotechnology Platform Program" of the Ministry of Education, Culture, Sports, Science and Technology (MEXT), Japan.

References

1 C. Nylander, B. Liedberg, and T. Lind: Sens. Actuators **3** (1982/83) 79. http://dx.doi.org/10.1016/0250-6874(82)80008-5
2 T. Liebermann and W. Knoll: Coll. Surf. A **171** (2000) 115. https://doi.org/10.1016/S0927-7757(99)00550-6
3 J. N. Anker, W. P. Hall, O. Lyandres, N. C. Shah, J. Zhao, and R. P. van Duyne: Nat. Mater. **7** (2008) 442. https://doi.org/10.1038/nmat2162
4 M. T. van Os, B. Menges, R. Foerch, G. J. Vancso, and W. Knoll: Chem. Mater. **11** (1999) 3252. https://doi.org/10.1021/cm991068k
5 K. Sato, Y. Ohki, K. Nomura, M. Fujimaki, and K. Awazu: Nanotechnol. **22** (2011) 245503. https://doi.org/10.1088/0957-4484/22/24/245503
6 M. Yasuura and M. Fujimaki: Sens. Mater. **31** (2019) 63. https://doi.org/10.18494/SAM.2019.2044
7 C. Kuroda, Y. Ohki, and M. Fujimaki: Opt. Express **25** (2017) 26011. https://doi.org/10.1364/OE.25.026011
8 C. Kuroda, M. Nakai, M. Fujimaki, and Y. Ohki: Opt. Express **26** (2018) 6796. https://doi.org/10.1364/OE.26.006796
9 M. Fujimaki, C. Rockstuhl, X. Wang, K. Awazu, J. Tominaga, Y. Koganezawa, Y. Ohki, and T. Komatsubara: Opt. Express **16** (2008) 6408. https://doi.org/10.1364/OE.16.006408
10 X. Wang, M. Fujimaki, T. Kato, K. Nomura, K. Awazu, and Y. Ohki: Opt. Express **19** (2011) 20205. https://doi.org/10.1364/OE.19.020205
11 M. Fujimaki, X. Wang, T. Kato, K. Awazu, and Y. Ohki: Opt. Express **23** (2015) 10925. https://doi.org/10.1364/OE.23.010925
12 S. C. B. Gopinath, K. Awazu, M. Fujimaki, and K. Shimizu: Acta Biomaterialia **9** (2013) 5080. https://doi.org/10.1016/j.actbio.2012.09.027

13 S. C. B. Gopinath, K. Awazu, M. Fujimaki, K. Shimizu, and T. Shima: PLoS ONE **8** (2013) e69121. https://doi.org/10.1371/journal.pone.0069121
14 H. Ashiba, M. Fujimaki, K. Awazu, M. Fu, Y. Ohki, T. Tanaka, and M. Makishima: Sensing and Bio-Sensing Research **3** (2015) 59. https://doi.org/10.1016/j.sbsr.2014.12.003
15 H. Ashiba, M. Fujimaki, K. Awazu, M. Fu, Y. Ohki, T. Tanaka, and M. Makishima: Jpn. J. Appl. Phys. **55** (2016) 027002. http://doi.org/10.7567/JJAP.55.027002
16 F. Demichelis, A. Tagliaferro, E. Tresso, and P. Rava: J. Appl. Phys. **57** (1985) 5424. https://doi.org/10.1063/1.334867
17 H. Makihara, A. Tabata, Y. Suzuoki, and T. Mizutani: Vacuum **59** (2000) 785. https://doi.org/10.1016/S0042-207X(00)00348-1
18 C. Goncalves, S. Charvet, A. Zeinert, M. Clin, and K. Zellama: Thin Solid Films **403–404** (2002) 91. https://doi.org/10.1016/S0040-6090(01)01553-X
19 D. T. Pierce and W. E. Spicer: Phys. Rev. B **5** (1972) 3017. https://doi.org/10.1103/PhysRevB.5.3017
20 H. Hwang, M. G. Park, H. Ruh, and H. Yu, Bull: Korean Chem. Soc. **31** (2010) 2909. https://doi.org/10.5012/bkcs.2010.31.10.2909
21 E. D. Palik: Handbook of Optical Constants of Solids I, II & III (San Diego, CA Academic, 1998)
22 M. Born and E. Wolf: Principles of Optics: Electromagnetic Theory of Propagation, Interference and Diffraction of Light 6th ed. (Reprinted, with corrections) (Pergamon Ltd., 1986).